Fizika Nizkikh Temperatur, 2010, v. 36, Nos. 10/11, p. 1107–1116

Superconductor–insulator transitions of quench-condensed films

A.M. Goldman

School of Physics and Astronomy, University of Minnesota, 116 Church Str., SE, Minneapolis MN 55455, USA
E-mail: goldman@physics.umn.edu

Received April 1, 2010

The superconductor–insulator transitions of quench-condensed ultrathin films of metals are simple examples of continuous quantum phase transitions. Quantum phase transitions differ from thermal phase transitions in that they occur at zero temperature when the ground state of a system is changed in response to a variation of an external parameter of the Hamiltonian. In superconductor–insulator transitions, this control parameter is usually parallel or perpendicular magnetic field, disorder, or charge density. Quantum phase transitions are studied through measurements at nonzero temperature of physical behaviors influenced by the quantum fluctuations associated with the transition. Here we will focus on the results of transport and magnetotransport measurements of disordered quench-condensed films of metals that are effectively two-dimensional. Open questions relating to the nature of the very puzzling insulating regime and whether there are several different types of superconductor-insulator transitions determined by material properties will be presented.

PACS: 74.40.Kb Quantum critical phenomena;
74.40.Gh Nonequilibrium superconductivity;
74.62.En Effects of disorder;
74.78.–w Superconducting films and low-dimensional structures.

Keywords: superconductor–insulator transition, quench-condensed films.

1. Introduction

Interest in two-dimensional (2D) superconductivity, which is the starting point for this research, began with proposals by Ginzburg and Kirzhnits [1] to the effect that superconductivity might occur at elevated temperatures in such systems. The specific configuration proposed was that of electrons in surface energy states. Recent studies of interfacial phenomena in oxides seem to provide a realization of this idea albeit at very low temperatures [2]. The net consequence of the Ginzburg–Kirzhnits proposal was the initiation of substantial research on the properties of very thin films which has led to substantial new physics, but thus far no discovery of high temperature superconductivity.

The study of 2D systems has been a mainstay of the investigation of fluctuation phenomena in superconductors. This took place in two stages: the first involved the investigation of precursive superconductivity the highlight of which was the establishment of the validity of the Aslamazov–Larkin theory of the superconducting fluctuation contribution to the conductivity of the normal state. (For a review see Larkin and Varmalov [3].) Sometime later, in the context of the properties of superfluid helium and 2D melting, it was established that long-range order in 2D could be topological, or quasi-long range in the case of the *XY* model universality class [4]. Afterwards it was realized that the effective penetration length of 2D superconductors could be a macroscopic length. As a consequence Abrikosov vortices in the 2D limit could interact logarithmically and the transition to the superconducting state in 2D, itself could be a topological phase transition [5]. This led to another stage of investigations of 2D superconductivity, an activity that continues to this day in part because the cuprate high temperature superconductors are effectively layered compounds involving coupled or weakly coupled 2D layers [6].

Another stream in the evolution of the subject was the realization that disorder was an important element in determining the properties of 2D superconductors. Magnetic impurities are pair breaking, but nonmagnetic impurities were predicted to not have a deleterious impact on superconducting pairing. This is known as Anderson's theorem [7,8]. On the other hand, with a high enough level of disorder, Anderson localization will occur [9]. Under strong

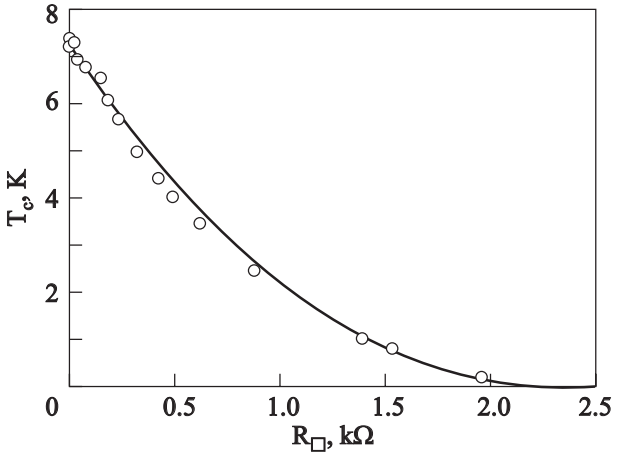

Fig. 1. Suppression of superconductivity in amorphous $MoGe_x$ with increasing disorder adapted from Graybeal and Beasley. The solid line is a theoretical fit as proposed by Finkel'stein.

conditions of electron localization, superconductivity should disappear even with an attractive interaction [10]. This led to investigations of the dependence of transition temperatures on sheet resistances. The fundamental idea was that disorder reduces the screening of the electron–electron repulsion and the electronic density of states, leading to a net weakening of the electron–electron attractive interaction and superconductivity. Figure 1 shows the data of Graybeal and Beasley [11] on the reduction of the transition temperature of $MoGe_x$ films with increasing sheet resistance or disorder.

The solid line is generated by a theory due to Finkel'shtein [12]. This model, which effectively describes the reduction of the transition temperature, should not work in the limit of really strong disorder. The reason for this is that as the transition temperature is driven towards zero temperature, fluctuations increase and eventually become quantum mechanical. This raises the issue as to whether the endpoint of the reduction of the transition temperature is a quantum critical point, with disorder controlling the ground state of the system.

The first indication that disorder might drive the transition temperature low enough that quantum fluctuations could be important was the work of Haviland, Liu, and Goldman [14] in which the thickness variation of $R(T)$ was studied in amorphous Bismuth (*a*-Bi) films. This investigation was carried out using an apparatus in which films could be grown in situ at low temperatures and measurements carried out alternating with increments of growth. Bismuth is a semimetal in crystalline form, but is metallic under high pressure and in thin film amorphous form. The latter results when Bi films are grown on substrates held at liquid helium temperatures [13]. Curves of $R(T)$ for a set of *a*-Bi films are shown in Fig. 2 [14].

These resemble renormalization flows to an unstable fixed point at zero temperature. For this particular set of films its value corresponds to the quantum resistance for

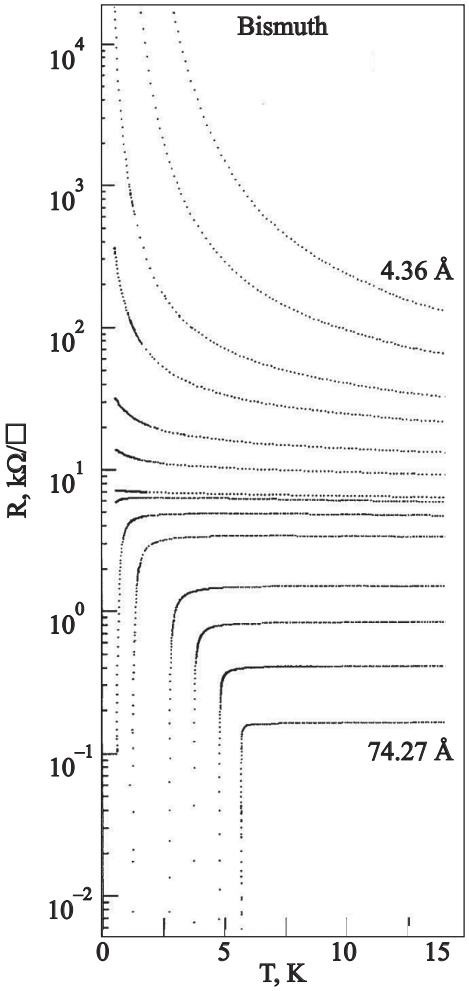

Fig. 2. Evolution of the temperature dependence of the sheet resistance $R(T)$ with thickness for an *a*-Bi film deosited onto *a*-Ge. Fewer than half of the traces actually acquired are shown. Film thicknesses that are shown range from 4.36 to 74.27 Å from top to bottom.

pairs, $h/4e^2$, which is approximately 6450 Ω. This result set the stage for consideration of the SI transition as a continuous quantum phase transition [15].

2. Quantum phase transitions

Quantum phase transitions are transitions that take place at absolute zero, where the crossing of the phase boundary changes the quantum mechanical ground state. The control parameter, rather than being temperature, is some parameter of the Hamiltonian of the system. For 2D superconducting films the parameter could be disorder, perpendicular or parallel magnetic field, or charge density. (For a review see: Goldman and Marković [16].) The understanding of such transitions requires that quantum effects need to be considered. This is to be contrasted with nonzero temperature transitions, which in some sense are classical even though the underlying microscopic physics is quantum mechanical. The reason for this is that although quantum fluctuations for such transitions may be important

at microscopic length scales, they are not relevant at the longer length scales that are associated with critical behavior. Critical fluctuations can be understood in the context of classical statistical mechanics with an effective Hamiltonian for the order parameter given by the Landau free-energy functional.

Continuous phase transitions at zero temperature are accompanied by divergent correlation lengths and times. (For a relatively elementary discussion see: Sondhi et al. [17].) The frequency associated with critical fluctuations vanishes as the transition temperature. The system, and the critical fluctuations, will behave classically whenever the energy associated with them is less than $k_B T$. In the limit of zero temperature this is not the case, so the fluctuations behave quantum mechanically. Usually the correlation length is written as

$$\xi = \xi_0 |t|^{-\nu} \tag{1}$$

where ν is the correlation length exponent and t is the reduced temperature $t = |T - T_c / T_c|$. Similarly the relaxation time of the order parameter in the critical regime is given by

$$\tau \sim \xi^z . \tag{2}$$

Here z is the dynamical critical exponent. Usually τ is denoted as ξ_τ, which is called the dynamical correlation length. In the general case, and specifically for zero-temperature phase transitions, t is replace by δ , which is a dimensionless distance from a transition point which could be controlled by magnetic field strength, disorder, or charge density in the systems we are considering. For the example of the magnetic field-tuned transition, $\delta = |(B - B_c) / B_c|$ With these definitions we can write

$$\xi_\tau \sim |\delta|^{-\nu z} . \tag{3}$$

It is well known that the statistical physics problem of a zero temperature d -dimensional system at $T = 0$ can be reduced to a classical problem whose effective dimension equals $d + z$ [17]. The quantum mechanical partition function looks like a classical partition function in $d + z$ dimensions. When $z = 1$, which is believed to be the case for systems with long range interactions, the extra dimension is finite in extent and is given by $-i\hbar\beta$ in units of imaginary time. In the $T \Rightarrow 0$ limit this length diverges, and the effective dimension is $d + 1$. This means that the zero temperature limit of a 2D system at finite temperatures such as the 2D *XY* model would have an effective dimension of 3.

Fisher presented a scaling form that can be used to characterize properties measured at nonzero temperatures in the regime of critical fluctuations and to thus determine the critical exponents and universality class of the transition [18]. For the resistance near the transition, the scaling function is of the form:

$$R = R_c F\left(\delta / T^{1/\upsilon z}, \delta / E^{1/\upsilon(z+1)}\right). \tag{4}$$

Here R is the sheet resistance, R_c and F are an arbitrary constant and an arbitrary function respectively. The energy scale for the fluctuations $\Omega \sim \xi_\tau^{-z}$, is cut off at nonzero temperature by $k_B T$, defining a cut off length L_T given by $k_B T \sim L_T^{-z}$ This gives rise to the first term in the argument of the arbitrary function *F*. The second term comes from a characteristic length associated with the electric field as compared with the correlation length.

The applicability of these ideas assumes that there is a continuous and direct superconductor–insulator (SI) transition controlled by a parameter of the Hamiltonian such as perpendicular or parallel magnetic field, disorder, or charge transfer. The first scaling analysis of perpendicular field driven transition was carried out by Hebard and Palaanen [19] on InO_x films. They found that the exponent product $\nu z \sim 1.2$ from scaling with only the first argument of Eq. (4). Later Yazdani and Kapitulnik [20] analyzed the properties of $MoGe_x$ films, carrying out both temperature and electric field scaling. They determined both z and $z + 1$ and thus concluded that $z = 1$ in agreement with expectations [21]. This will be discussed further in Sec. 6.

The relevance of Eq. (4) to the actual behavior of films depends upon whether there is a direct continuous, SI transition, independent of the underlying mechanism for the transition. For direct transitions there are two distinctive schools of thought. One approach has the insulating behavior resulting from the localization of charged Bosons, i.e., Cooper pairs [18,22]. The second has the insulator resulting from the localization of Fermions that result from the enhancement of Coulomb repulsion that suppresses pairing [12]. There is substantial evidence to support this latter view [23]. There are also ideas [24,25] and some experimental evidence [26] for an indirect transition in which there is an intermediate inhomogeneous phase in which a film contains superconducting and insulating puddles. There is also some evidence for an intermediate metallic regime [27]. It is clear that there may be several types of SI transitions, depending upon the material, its level of disorder and the specific control parameter.

In the following we will consider a series of investigations of SI transitions in films of *a*-Bi, all of which are very close to the disorder-tuned SI transition of Fig. 1. In all of the cases considered, the transition appears to be direct, and it was possible to carry out a scaling analysis using the first argument of Eq. (4) with the in-plane electric field fixed and the *I–V* characteristic in the linear regime. An important caveat is that the success of scaling by itself and the identification of the universality class of the transition from the values of the critical exponents may not elucidate the microscopic physics of the transition or the nature of the insulating state.

3. Experimental approach

The films that were investigated were grown on substrates held at or near liquid helium temperatures. Single-crystals of (100) $SrTiO_3$ served as substrates. Platinum electrodes, 100 Å thick, configured for four-terminal electrical measurements were pre-evaporated onto the epi-polished front surfaces of the substrates. Experiments were initiated with the placement of the substrate in a dilution refrigerator/UHV deposition apparatus. In the early work this was an SHE minifridge [28]. In later work an Oxford Kelvinox 400 dilution refrigerator was employed [29]. Films were grown by first depositing a 10 Å thick underlayer of *a*-Ge or *a*-Sb, followed by subsequent layers of *a*-Bi. All depositions were carried out under UHV conditions with the substrates held at or near liquid-helium temperatures during deposition. The geometry of the positions of the sources relative to the substrates in the two different setups was identical. In the apparatus that employed the minfridge, the cryostat was moved in and out of the growth chamber, whereas in that employing the Kelvinox 400 the substrates were held on a helium-cooled transfer rod which was used to move samples on and off the refrigerator platform, and in and out of the growth chamber. Films grown at liquid helium temperatures with the indicated underlayers are believed to be homogeneously disordered [30]. This approach allows for repeated cycles of in situ evaporation and measurement permitting the generation of curves of $R(T)$ at different thicknesses as shown in Fig. 2.

4. Thickness- and perpendicular magnetic field-tuned SI transitions

We now consider data of $R(T,\delta)$ for a set of films different from those shown in Fig. 2. As is typical of such experiments, at some critical thickness, d_c, R becomes effectively temperature independent, while for even thicker films it decreases rapidly with decreasing temperature, indicating the onset of superconductivity. The critical thickness is found by plotting R vs. d at different temperatures (inset of Fig. 3) and identifying the crossing point for which the resistance is temperature independent, or by plotting dR/dT vs. d at the lowest temperatures and finding the thickness for which $dR/dT \Rightarrow 0$.

In the quantum critical regime the resistance of a two-dimensional system is expected to obey the scaling law of Eq. (4), with the in-plane electric field taken to be a constant and with current-voltage characteristics in the linear regime.

To analyze the data, we obtain curves of R vs. d at various temperatures. Having determined the critical thickness in the manner described above, we then rewrite Eq. (4) as $R(t,\delta) = R_c F(\delta t)$, where $t = T^{-1/\upsilon z}$ and we have dropped the dependence on E. The parameter $t(T)$ is treated as an unknown variable which is determined at each temperature to obtain the best collapse of the data.

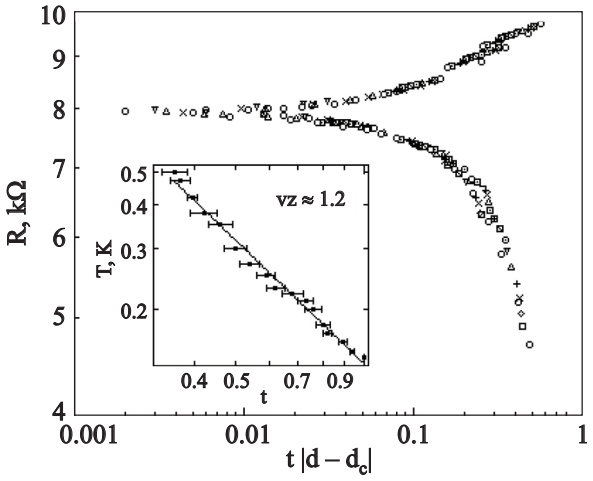

Fig. 3. Resistance per square as a function of the scaling variable, $t|d-d_c|$, for seventeen different temperatures, ranging from 0.14 to 0.5 K. Different symbols represent different temperatures. Te inset shows the temperature dependence of t.

Specifically, t is determined by performing a numerical minimization between a curve at a particular temperature and the lowest temperature curve. The exponent product υz is then found from the temperature dependence of t, which must be a power law in temperature for the procedure to make physical sense. This procedure does not require either detailed knowledge of the functional form of the temperature or thickness dependence of R, or prior knowledge of the critical exponents.

A different method of obtaining critical exponents was also used to check the consistency of this procedure. A log–log plot of $(\partial R/\partial d)|_{d_c}$ vs. T^{-1} was constructed. Its slope is equal to $1/\upsilon z$ if Eq. (4) is obeyed. Exponents obtained using the two approaches were essentially identical, within the quoted experimental uncertainty. The collapse of the data of $R(t,\delta)$ is shown in Fig. 3 [31]. The exponent product υz is found to be 1.2 ± 0.2 with the error determined from the power law fit.

In addition, the magnetoresistance as a function of temperature and perpendicular magnetic field with perpendicular field orientation was also studied. By sorting this data the perpendicular field tuned transition in a nonzero magnetic field can be investigated. A scaling analysis resulted in a critical exponent product of 1.4 ± 0.2 apparently independent of magnetic field.

Values of $R(T)$ for five films of different thickness were studied in magnetic fields of up to 1.2 T, applied perpendicular to the plane. The exponent product was determined with magnetic field rather than thickness as the tuning parameter. The collapse of the data in this instance is shown in Fig. 4.

The exponent product determined in a similar manner was found to be $\upsilon z = 0.7 \pm 0.2$ for each of the five films. The same value was obtained from log- log plots of the derivative at the critical field vs. T^{-1}. The fact that the

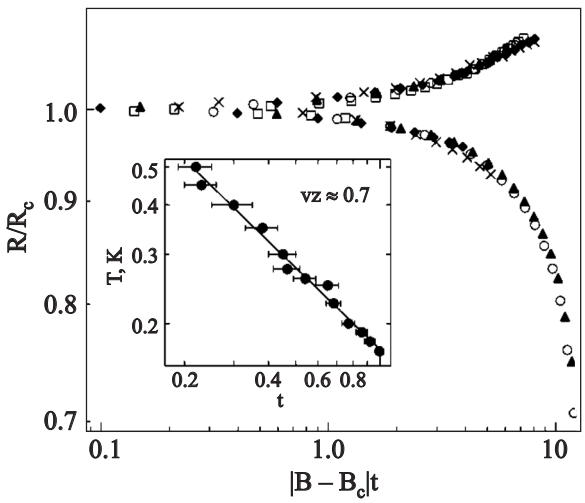

Fig. 4. Normalized resistance per square as a function of the scaling variable $t|B-B_c|$. Each symbol represents one film at different temperatures. Only a small portion of the data is shown for clarity. Inset. The fitting parameter t determines the value of υz.

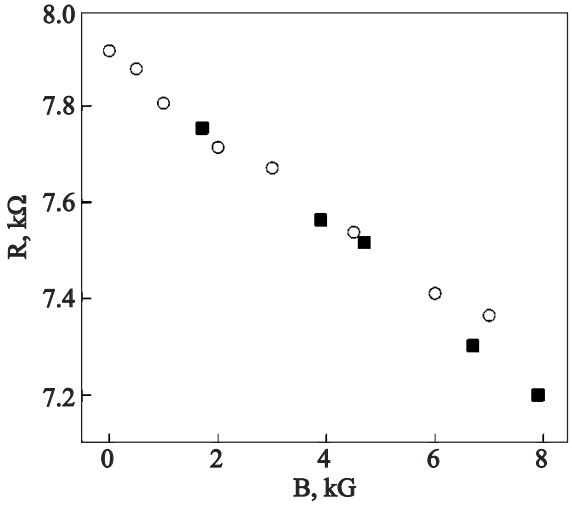

Fig. 6. The critical resistance as a function of the critical field for a series of bismuth films. Here R_c decreases with increasing thickness, as thicker films have lower normal-state resistances and higher critical fields.

exponent product differs from that of the thickness tuned transition suggests a universality class different from that of the thickness-tuned transition. It is possible to combine the data obtained from the thickness-tuned transitions in fixed magnetic field and field-tuned transitions at fixed thickness to construct a phase diagram with thickness and magnetic field as independent variables. This is shown in Fig. 5. The films characterized by parameters which lie above the boundary are insulating and those below are superconducting, distinguished by the sign of dr/dT.

The critical resistance, in contrast with the predictions of the dirty Boson model, is not universal. Figure 6 shows that it decrease as the field increases, roughly in a linear fashion. Thicker films have lower normal-state resistances and higher critical fields, this means that T_c increases with increasing thickness. Variants of the dirty Boson model predict values of the critical resistance close to those found here.

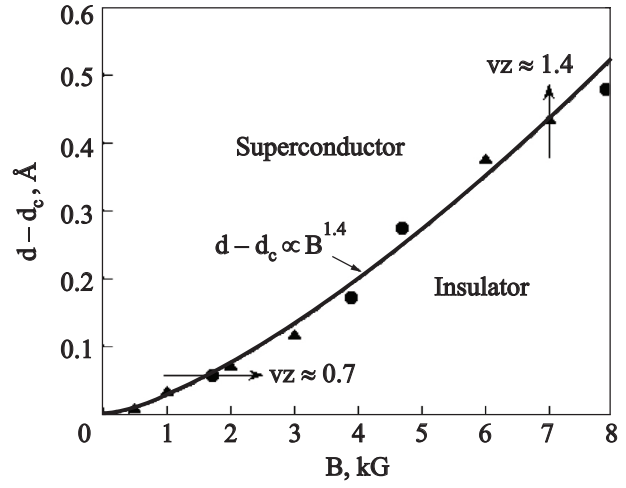

Fig. 5. Phase diagram in the $d-B$ plane in the $T \Rightarrow 0$ limit. The points on the phase boundary were obtained from disorder-driven transitions (triangles) and magnetic-field-driven transitions (circles). Values of the critical exponent products are shown next to arrows giving the direction in which the boundary was crossed. Here dc is the zero-eld critical thickness.

It is important to note several features of these two different SI transitions. The transitions are direct in that there appear to be no intermediate metallic phases and there is no resistance saturation at the lowest temperatures. This is in contrast with results reported for other types of systems [27,32], or what is found in granular films [33]. It should also be noted that the films which have been studied in the case of the perpendicular field tuned SI transition are very close in their properties to the insulating regime. Subsequent works, in our laboratory on *a*-Bi films [34], and by others on *a*-Pb films [35], with resistances well below that of the critical resistance of the thickness-tuned transition have revealed the presence of an intermediate regime that may have two phases. The precise nature of the crossover from direct transitions near criticality to indirect transitions with decreasing disorder (resistance) is not known.

5. Parallel magnetic field tuned SI transition

The superconductor-insulator transition of a-Bi films was studied in parallel magnetic fields in two types of samples, those in which superconductivity was induced by electrostatic doping, which will be discussed below, and those which were intrinsic superconductors with thicknesses close to the critical thickness for the appearance of superconductivity [36]. In the case of a 10.22 Å thick film induced into the superconducting state with a charge (electron) transfer of $3.35{\cdot}10^{13}$ cm^{-2}, the best collapse of the data was with $\upsilon z = 0.65 \pm 0.1$. The results of the scaling analysis are shown in Fig. 7.

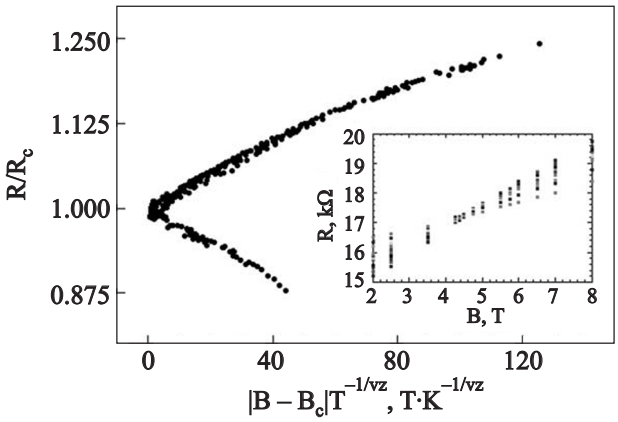

Fig. 7. Finite size (temperature) scaling plot for a 10.22 Å thick film with $\Delta n = 3.35 \cdot 10^{13}$ cm^{-2} with B as the tuning parameter. Data included is over the range from 150 to 340 mK. The best collapse was achieved with $\upsilon z = 0.65 \pm 0.1$. Inset: isotherms of $R(B)$ at temperatures between 150 and 340 mK.

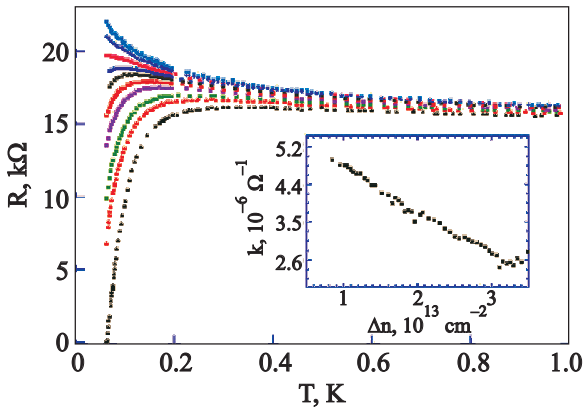

Fig. 8. Resistance vs. temperature, $R(T)$, at various values of Δn for a 10.22 Å thick film with $B = 0$. Data are shown from 60 mK to 1 K. The values of Δn that are shown, from top to bottom, are 0, 0.62, 1.13, 1.43, 1.61, 1.83, 2.04, 2.37, 2.63, and $3.35 \cdot 10^{13}$ cm^{-2}. Forty four curves of $R(T)$ for other values of Δn are omitted from the plot for clarity. Inset: slope of $\ln(T)$ vs. Δn.

The results of a similar study of an intrinsically superconducting film 10.25 Å thick were nearly identical. A distinct crossing point was found with $R_c = 10460\ \Omega$ and $B_c = 9.18$ T. The exponent product that produced the best collapse of data was 0.75 ± 0.1, slightly higher than that found for the field-tuned transition of an electrostatically induced superconducting film, but agreeing within the uncertainty of the analysis.

6. Electrostatic control of the SI transition

Since there may be issues of sample inhomogeneity and variable strength vortex pinning in thickness- and perpendicular magnetic field-tuned transitions, it is of interest to study SI transitions in which the level of physical disorder is fixed, and in which the outcome of the study is not dependent upon the degree of vortex pinning. This can be accomplished by inducing superconductivity in an insulator using the electric field effect [37]. The presumption is that the same level of disorder is present in the insulating and superconducting states. The field effect geometry was one in which $SrTiO_3$ (STO) crystal served as both a substrate and gate insulator. The preparation of this device involved several steps. First a small section of the unpolished back surface of a 500 μm thick single crystal of (100) STO was mechanically thinned *ex situ*, resulting in this surface and the epi-polished front surface being parallel and separated by 45 ± 5 μm [38]. A 0.5×0.5 mm, 1000 Å thick, Pt gate electrode was then deposited *ex situ* onto the thinned section of the back surface directly opposite the eventual location of the measured square of film. Platinum electrodes, 100 Å thick were also deposited *ex situ* onto the substrates polished front surface to form a four-probe measurement geometry. After the substrate was placed in the dilution refrigerator, a 10 Å thick underlayer of *a*-Sb and successive layers of *a*-Bi were deposited through a shadow mask onto the substrate's front surface under UHV conditions. A sequence of *a*-Bi films was studied [36,39]. The temperature dependence of insulating films was governed by the 2D Mott variable range hopping form:

$$R(T) = R_0 \exp\left[(T_0/T)^{1/3}\right]. \qquad (5)$$

In the case of an insulating film, 10.22 Å in thickness, the addition of electrons to the film, using the field effect, induced superconductivity. The evolution of this electrostatically tuned SI transition with charge transfer is shown in Fig. 8. An important feature of the data was the crossover from Mott hopping in the insulating regime to a $\ln(T)$ dependence of the conductance on temperature in the normal state for films which underwent a transition to superconductivity. What was also found is that the slope of the $\ln(T)$ term in the conductance was a linear function of the charge transfer, as shown in the inset to Fig. 8.

This SI transition, as shown in Fig. 9 was successfully analyzed using temperature scaling [17], employing the charge transfer Δn as the control parameter. This strongly suggests that the electrostatically tuned transition is also a continuous quantum phase transition. In this instance, the exponent product υz was 0.7 ± 0.1 all the way up to 1 K provided that the $\ln(T)$ dependence of the conductance was first removed. This was done by assuming that the electron interactions were independent of the critical fluctuations.

The electrostatically tuned SI transition appears to involve little change in physical disorder as determined by noting that the resistance above 1 K changes very little as

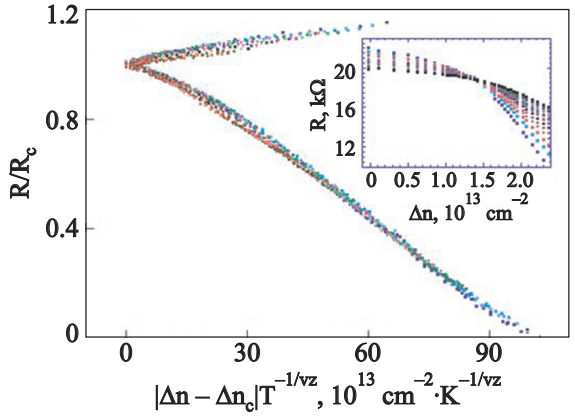

Fig. 9. Finite size scaling plot for a 10.22 Å thick film with $B = 0$, including data from 60 to 140 mK with Δn as the tuning parameter. Fifty four values of Δn between 0 and $3.35 \cdot 10^{13}$ have been included. The best collapse of the data was for $\upsilon z = 0.7$ with an uncertainty of ± 0.1. Inset: $R(\Delta n)$ for isotherms between 60 and 140 mK. If the $\ln T$ dependence of the normal state resistance is taken out of the superconducting films, the scaling can be extended up to 1 K.

superconductivity develops. This is in contrast with what is found for the disorder or thickness tuned transition. In Fig. 10 we show the resistances at 120 mK as a function of the resistances at 1 K for the electrostatic and thickness-tuned transitions. The thickness-tuned transition takes place with a much larger change in the high temperature resistance than does the electrostatically tuned transition. The apparent coincidence of an insulator–metal transition with the insulator–superconductor transition suggests that the charge-tuned SI transition is a Fermionic phenomenon and is not associated with the localization of Bosons.

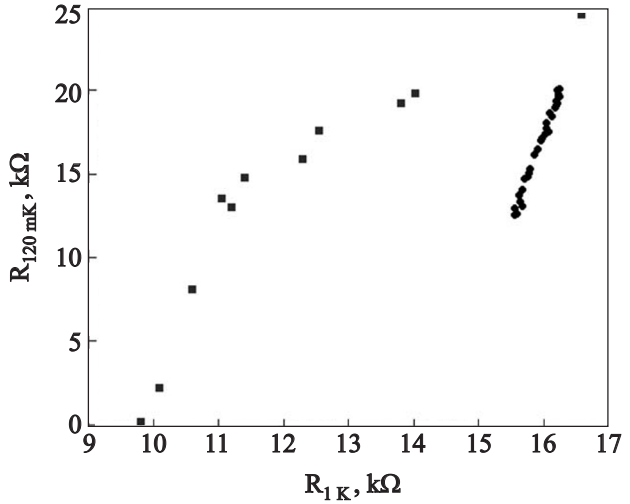

Fig. 10. Resistance at 1 K as a function of resistance at 120 mK for electrostatic (circles) and thickness (squares) tuned SI transitions. As superconductivity develops, the resistance at 1 K changes much more for thickness tuning than for electrostatic tuning.

7. Nonlinear and hot electron effects

The nature of a quantum phase transition is determined by the values of the correlation length exponent and the dynamical critical exponent, respectively. Nonlinear conductivity near the quantum critical point can be important because the results of a finite size scaling analysis under changes of in-plane electric field can be combined with scaling under changes of temperature to determine separate values of the two exponents. In this analysis, it is important to determine the extent to which intrinsic nonlinear response is more important than Joule heating [17]. It has been possible to demonstrate that the dominant effect in *a*-Bi films is actually electron heating. An electric field scaling analysis of *a*-Bi films that successfully collapses data has been shown to be a direct consequence of heating and not a quantum critical nonlinear electric response. This is a consequence of being able to map electric field scaling onto temperature scaling by relating in-plane electric fields (voltages) and the resultant nonlinear current response to elevated electron temperatures.

Figure 11 shows differential resistance vs. measuring current for a parallel field tuned SI transition of an *a*-Bi film. The value of R_D / R_{D_c} is plotted as a function of $|B - B_c| V^{-1/\upsilon(z+1)}$ where V is the in-plane voltage across the film.

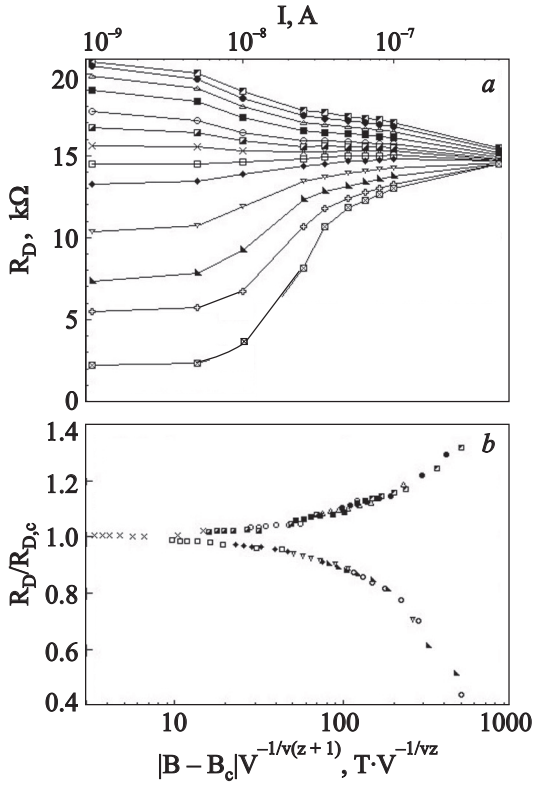

Fig. 11. a — differential resistance vs. measurement current for a parallel magnetic field tuned transition. From bottom to top the magnetic fields are 2, 3, 4, 5, 6, 6.5, 7, 7.5, 8, 9, 10, 1, and 12 T. *b* — electric field scaling for the data of (*a*).

The result of the temperature scaling, which is not shown, is $\upsilon z = 0.68 \pm 0.05$ whereas for the electric field scaling; $\upsilon(z+1) \sim 2$. This then yields $z \sim 0.5$ and $\upsilon \sim 1.3$ [40]. The resultant value of z is believed to be unphysical as it should be 1 or 2 for charged Bose systems, depending upon their interactions [21].

After detailed scrutiny of the variation of the differential resistance with temperature and magnetic field, it was seen that values of $R_D(T)$ with decreasing temperature become temperature independent at particular values of current. This suggests that these currents heat the electrons to the particular temperature for all lower refrigerator temperatures. Upon quantitative analysis of this hypothesis it is found that $T_{\text{electron}} \sim P^{0.18}$ where P is the power dissipated in the film by the current. This is very close to the relationship proposed by Wellstood et al. [41] to describe the relationship between a disordered metal film's minimum electron temperature as measured using Johnson noise, and measurement power.

The result is that electric field scaling can be mapped onto temperature scaling and for the particular a Bi film in question leads to $\upsilon z = 0.72$ which agrees within experimental uncertainty with the value obtained by temperature scaling. Electric field scaling then appears to work because it is really temperature scaling and the increased measurement current to enter the nonlinear regime simply heats the electrons [40].

An important question is whether this is a general result. In the zero temperature limit, nonlinear transport effects are expected to compete with Joule heating with material-specific properties being important. The electron temperature varies with power as $T_{\text{electron}} \sim P^{1/\theta}$ with $\theta = p + 2$ where p is the power of the temperature in the expression for the temperature dependence of the inelastic electron-phonon scattering rate, $\tau_{\text{in}}^{-1} \sim T^p$. There is a criterion that for $2/\theta < z/(z+1)$, Joule heating rather than intrinsic nonlinear effects will dominate [17]. This criterion arises from a dimensional analysis that may ignore important multiplicative factors. Assuming z to be 1 or 2, the value of θ for *a*-Bi meets this criterion. However, even in the earlier work of Yazdani and Kapitulnik [20] on $MoGe_x$ thin films, in which scaling analyses revealed apparent values of $\upsilon z \sim 1.35$ and $\upsilon(z+1) \sim 2.65$, leading to $\upsilon \sim 1.3$ and $z \sim 1$, heating may actually be responsible. It is known that $p = 2$ in $MoGe_x$, so that $\theta = 4$. This puts $MoGe_x$ in the marginally «dangerous» category in which both heating and intrinsic fluctuation effects may be important. With the particular value of p for this material, one can also map electric field scaling onto temperature scaling. The resultant conclusion from all of this is that measuring currents can heat electrons out of equilibrium with their environment. This prevents electric field scaling from yielding information allowing the separate determination of υ and z. Because this analysis depends upon material parameters it is possible that there exist materials for which this analysis would work.

8. Discussion

In the above we have reviewed the results of a series of investigations of SI transitions of quench-condensed films tuned by disorder (thickness), parallel and perpendicular magnetic fields, and electrostatic charging. All of these examples have exhibited direct SI transitions. In all but the case of thickness the exponent products have been $\upsilon z \sim 0.7$ within experimental error, a value very close to what might be expected for a 2D *XY* model if the dynamical exponent $z = 1$, or the Bose–Hubbard model without disorder. The films studied in each instance were either superconducting, with resistances very close to the critical resistance for the thickness tuned transition, or insulating, in the case of the electrostatically induced transition, with resistances again very close to the critical resistance.

There was no evidence of metallic regimes at low temperatures near criticality. The Bose–Hubbard model of the SI transition in 2D predicts a metallic ground state only at the critical value of the tuning parameter. In experiments reported by others, temperature independent resistances have been found on both sides of the SI transition over an extended range of tuning parameters [27,32]. The nature of this resistance saturation is far from certain because of specific difficulties with electrical measurements at milliKelvin temperatures. The electronic heat capacities and coupling of the electronic degrees of freedom to the heat bath are so weak that even modest levels of Joule heating may prevent cooling of films' electrons. A refrigerator could thus cool phonons more effectively than electrons resulting in a temperature independent resistance since the film would be measured at its minimum achievable electron temperature over an extended range of lower phonon or lattice temperatures.

Scaling of the thickness-tuned transition led to an exponent product $\nu z \sim 1.3$ which is very close to that found for the perpendicular field tuned transition of $MoGe_x$. Recently Steiner, Breznay and Kapitulnik (2008) reported the results of a study of perpendicular field tuned SI transitions, which combined data from Ta, $MoGe_x$, and InO_x films. It is claimed that InO_x films can be more disordered than $MoGe_x$ films and that there are two branches of properties, a low-disorder branch in which a scaling analysis leads to $z \sim 1$ and $\upsilon z \sim 1.35$, and a high disorder branch with $\upsilon \sim 7/3$, and near the intersection of the branches, $\upsilon \sim 4/3$, but with less accurate scaling, again taking $z = 1$. The scaling with $\upsilon z \sim 1.35$ they associate with classical percolation, and the scaling with $\upsilon \sim 7/3$ with quantum percolation. The phase diagram with the two branches is in the space of critical conductance and critical field normalized to $H_{c2}(0)$. The less disordered branch they assert exhibits and intermediate metallic regime,

whereas the disordered branch has a direct SI transition. It is claimed that the disordered branch exhibits a critical conductance equal to that expected for the quantum conductance of pairs. Also the films in the high disorder branch exhibit a large peak in magnetoresistance in the insulating regime, which has been described by others for InO_x and TiN [47] films. Similar results have not been reported for any homogeneous metallic films grown by quench condensation.

One may ask, why the difference in behavior. It should be noted that in situ evaporated films of metals (*a*-Bi, *a*-Pb, and *a*-Be) are significantly thinner ($\sim$ 10 to 20 Å) than the InO_x, $MoGe_x$, or even TiN films (30 to 300 Å) that have been studied by various groups. Although they may have similar sheet resistances in the normal state, and short mean free paths, the carrier concentrations of the quench-deposited films may be significantly higher. Also, although there have been studies of structure of the compound films that classify them as amorphous and homogeneous, the spatial variation of chemical composition is not known, and can this can affect the homogeneity of the pairing potential. Indeed, recent STM studies at 0.050 K of TiN films have revealed a spatially varying gap and even a pseudogap above T_c [48]. Whether this is a result of chemical disorder has not been established, but the data are reminiscent of similar studies of cuprates where local inhomogeneity plays a role.

In the case of the perpendicular field tuned transition of quench evaporated films, when the sheet resistance falls below about 4000 to 5000 Ω the transition is no longer direct [34,35], and there appears to be an extended region where at least a nonzero temperatures there appears to be a two-phase regime, possibly superconducting droplets in a nonsuperconducting matrix [24,25,49]. This has been found in both *a*-Bi [34] and *a*-Pb films [35]. Thicker Bi films $\sim$ 24 Å, behave as high-κ Type-II superconductors and undergo a superconductor to metal transition.

The causes of the differences in the data between low carrier density compounds exhibiting SI transitions and quench-evaporated metals are not understood. There are distinct differences in the behavior of these two types of systems which likely have their origins in differences in carrier density, and perhaps in the length scale of the disorder. With the exception of the thickness-tuned SI transition, which returns exponent products $\upsilon z \sim 1.3$, all of the scaling analyses of SI transitions of quench-condensed nominally homogeneous films, tuned by charge transfer, and perpendicular and parallel magnetic field, which are direct transitions, yield an exponent product $\upsilon z \sim 0.7$, and if $z = 1$ as is anticipated for systems with long range interactions. The exponent $\upsilon \sim 0.7$ is consistent with a 3D *XY* model. As discussed earlier, it is anticipated that systems exhibiting nonzero temperature continuous phase transitions, in the limit in which the transition is driven to zero temperature will acquire extra dimensions. Thus systems belonging to the 2D *XY* model universality class, such as 2D superconductors would be expected to undergo a continuous quantum phase transitions belonging to the 3D *XY* model if $z = 1$. Again as mentioned earlier, knowledge of the universality class of the phase transition does not imply knowledge of the microscopic model. Whereas the electrostatically tuned SI transition appears to involve a simultaneous transition between an insulator exhibiting Mott variable range hopping and a 2D quantum corrected metal, which would appear to be Fermionic, the field-tuned transitions are not susceptible to such simple interpretation, and their microscopic nature appears to be an open question.

Acknowledgments

The author would like to thank the US National Science Foundation for continuing support of this work. He would also like to thank the numerous students who have contributed, including Bradford Orr, Heinrich Jaeger, David Haviland, Ying Liu, Anthony Mack, Nina Marković, Catherine Christiansen, Luis Hernandez, Sarwa Tan, Kevin Parendo and Yen-Hsiang Lin. The writing of this manuscript was supported by the NSF under grant NSF/DMR-0854752.

1. V.L. Ginzburg and D.A. Kirzhnits, *Zh. Eksp. Teor. Fiz. (USSR)* **46**, 397 (1964).
2. K. Ueno, S. Nakamura, H. Shimotani, A. Ohtomo, N. Kimura, T. Nojima, H. Aoki, Y. Iwasa, and M. Kawasaki, *Nature Mater.* **7**, 855 (2008).
3. Anatoly Larkin and Andrei Varlamov, *Theory of Fluctuations in Superconductors*, Oxford University Press, New-York (2005).
4. J.M. Kosterlitz and D.J. Thouless, *J. Phys.* **C6,** 1181 (1973).
5. M.R. Beasley, J.E. Mooij, and T.P. Orlando, *Phys. Rev. Lett.* **42**, 1165 (1979).
6. Myles A. Steiner, G. Beobinger, and A. Kapitullnik, *Phys. Rev. Lett.* **94**, 107008.
7. P.W. Anderson, *J. Phys. Chem. Solids* **11**, 26 (1959).
8. A.A. Abrikosov and L.P. Gor'kov, *Zh. Eksp. Teor. Fiz. (USSR)* **36**, 319 (1959).
9. E. Abrahams, P.W. Anderson, D.C. Licciardello, and T.V. Ramakrishnan, *Phys. Rev. Lett.* **42**, 673 (1979).
10. H. Ebisawa, H. Fukuyama, and S. Maekawa, *J. Phys. Soc. Jpn.* **54**, 2257 (1985).
11. J.M. Graybeal and M.R. Beasley, *Phys. Rev.* **B29**, 4167 (1984).
12. A.M. Finkelstein, *Physica* **B197**, 636 (1994).
13. W. Buckel and R. Hilsch, *Z. Phys.* **138**, 109 (1954).
14. D.B. Haviland, Y. Liu, and A.M. Goldman, *Phys. Rev. Lett.* **62**, 2180 (1989).
15. Subir Sachdev, *Quantum Phase Transitions*, Cambridge University Press, Cambridge (1999).
16. A.M. Goldman and N. Marković, *Phys. Today* **51**, 39 (1998).

17. S.L. Sondhi, S.M. Girvin, J.P. Carini, and D. Shahar, *Rev. Mod. Phys.* **69**, 315 (1994).
18. Matthew P.A. Fisher, *Phys. Rev. Lett.* **65**, 923 (1990).
19. A.F. Hebard and M.A. Paalanen, *Phys. Rev. Lett.* **65**, 927 (1990).
20. Ali Yazdani and Aharon Kapitulnik, *Phys. Rev. Lett.* **74**, 3037 (1995).
21. Igor F. Herbut, *Phys. Rev. Lett*. **87**, 137004 (2001).
22. Matthew P.A. Fisher, G. Grinstein, and S.M. Girvin, *Phys. Rev. Lett.* **64**, 587 (1990).
23. J.M. Valles, Jr., R.C. Dynes, and J.P. Garno, *Phys. Rev. Lett.* **69**, 3567 (1992).
24. Yonatan Dubi, Yigal Meir, and Yshai Avishai, *Nature* **449**, 876 (2007).
25. B. Spivak, P. Oreto, and S.A. Kivelson, *Phys. Rev.* **B77**, 214523 (2008).
26. Carlos L. Vicente,Yongguang Qin, and Jongsoo Yoon, *Phys. Rev.* **B74**, 100507 (2006).
27. Y. Seo, Y. Qin, C.L. Vicente, K.S. Choi, and Jongsoo Yoon, *Phys. Rev. Lett.* **97**, 057005 (2005).
28. B.G. Orr and A.M. Goldman, *Rev. Sci. Instrum.* **56**, 1288 (1985).
29. L.M. Hernandez and A.M. Goldman, *Rev. Sci. Instrum.* **73**, 162 (2002).
30. M. Strongin, R.S. Thompson, O.F. Kammerer, and J.E. Crow, *Phys. Rev.* **B1**, 1078 (1970).
31. N. Markovic, C. Christiansen, A.M. Mack, W.H. Huber, and A.M. Goldman, *Phys. Rev.* **B60**, 4320 (1999).
32. Nadya Mason and Aharon Kapitulnik, *Phys. Rev.* **B64**, 060504(R) (2000).
33. H.M. Jaeger, D.B. Haviland, B.G. Orr, and A.M. Goldman, *Phys. Rev.* **B40**, 182 (1989)
34. Yen-Hsiang Lin and A.M. Goldman, *arXiv:1002.1720*.
35. J.S. Parker, D.E. Read, A. Kumar, and P Xiong, *Europhys. Lett.* **75**, 950 (2006).
36. Kevin A. Parendo, K.H. Sarwa B. Tan, and A.M. Goldman, *Phys. Rev.* **B73**, 174527 (2006).
37. C.H. Ahn, A. Bhattacharya, M. Di Ventra, J.N. Eckstein, C. Daniel Frisbie, M.E. Gershenson, A.M. Goldman, I.H. Inoue, J. Mannhart, Andrew Millis, Alberto F. Morpurgo, Douglas Natelson, and Jean-Marc Triscone, *Rev. Mod. Phys.* **78**, 1185 (2006).
38. A. Bhattacharya, M. Eblen-Zayas, N.E. Staley, and A.M. Goldman, *Appl. Phys. Lett.* **85**, 997 (2004).
39. Kevin A. Parendo, K.H. Sarwa B. Tan, A. Bhattacharya, M. Eblen-Zayas, N. Staley, and A.M. Goldman, *Phys. Rev. Lett.* **94**, 197004 (2005).
40. Kevin A. Parendo, K.H. Sarwa B. Tan, and A.M. Goldman, *Phys. Rev.* **B74**, 134517 (2006).
41. F.C. Wellstood, C. Urbina, and J. Clarke, *Phys. Rev.* **B49**, 5942 (1994).
42. M.A. Paalanen, A.F. Hebard, and R.R. Ruel, *Phys. Rev. Lett.* **69**, 1604 (1992).
43. V.F. Gantmakher, *Physics-Uspekhi* **41**, 211 (1998); V.F. Gantmakher, M.V. Golubkov, V.T. Dolgopolov, G.E. Tsydnuzhapov, and A. Shashkin, *Pis'ma Zh. Eksp. Teor. Fiz.* **71**, 231 (2000).
44. Myles A. Steiner, Nicholas P. Breznay, and Aharon Kapitulnik, *Phys. Rev.* **B77,** 212501 (2008).
45. G. Sambandamurthy, L.W. Engel, A. Johansson, E. Peled, and D. Shahar, *Phys. Rev. Lett.* **94**, 017003 (2005).
46. R.W. Crane, N.P. Armitage, A. Johansson, G. Sambandamurthy, D. Shahar, and G. Gruner, *Phys. Rev.* **B75**, 184530 (2007).
47. T.I. Baturina, C. Strunk, M.R. Baklanov, and A. Satta, *Phys. Rev. Lett.* **98**, 127003 (2007); T.I. Baturina, C. Strunk, M.R. Baklanov, and A. Satta, *Phys. Rev. Lett.* **99**, 257003 (2007).
48. B. Sacépé, C. Chapelier, T.I. Baturina, V.M. Vinokur, M.R. Baklanov, and M. Sanquer, *Phys. Rev. Lett.* **101**, 157006 (2008); B. Sacépé, C. Chapelier, T.I. Baturina, V.M. Vinokur, M.R. Baklanov, and M. Sanquer, *arXiv:0906.1193.*
49. Amit Ghosal, Mohit Randeria, and Nandini Trivedi, *Phys. Rev.* **B65**, 014501(2001).